PHYSICAL REVIEW B VOLUME 27, NUMBER 8 15 APRIL 1983

Two-dimensional electrons in a magnetic field. III. Many-body effects

Y. Shiwa and A. Isihara
Statistical Physics Laboratory, Department of Physics, State University of New York at Buffalo, Buffalo, New York, 14260
(Received 23 August 1982)

A many-body theory is given to show that the magnetic properties of a two-dimensional electron system are dependent on the filling factor γ_0^{-1} defined as the ratio of the ideal Fermi energy against the field energy. Explicit results are obtained for absolute zero and large values of this factor. The internal energy is evaluated explicitly in consideration of the ideal, first-order exchange and ring contributions. The result converges for all r_s because for the ring contribution no small-momentum-transfer assumption is made and for low densities a rigorous analytical continuation is adopted. When plotted against γ_0^{-1}, the internal energy shows parabolic variations in a periodic way until it approaches the average kinetic energy for large γ_0^{-1}. The ideal susceptibility shows zigzag changes characteristic of absolute zero when it is plotted against γ_0^{-1}. It is zero at $\gamma_0^{-1}=2m+1$, where it jumps from $-2m$ to $2(m+1)$, m being an integer. The Coulomb interaction suppresses the zigzag variations for small r_s and inverts the oscillating pattern at $r_s \sim 0.7$. The oscillations thereafter may be considered characteristic of a liquid state rather than a gaseous state as they are somewhat different from those for small r_s. The susceptibility is convergent for all r_s.

I. INTRODUCTION

The de Haas–van Alphen (dHvA) effect has been used very effectively in the determination of the Fermi surface of metals. Traditionally, information on Fermi surfaces has been obtained from frequency analyses of the oscillating susceptibility based on the ideal-gas theories of Onsager and of Lifshitz and Kosevich.[1] However, since around 1970 it has been revealed that the amplitude of the oscillating susceptibility deviates from the ideal-gas formula. Such a deviation indicates that information concerning nonideality can be obtained from amplitude analyses. In 1971 Ishihara, Tsai, and Wadati[1] extended the ideal-gas theory to the interacting case and derived a microscopic expression which represents an exponential reduction of the amplitude due to electron interaction.

On the other hand, it has been found that quasi-two-dimensional electron systems in inversion layers of metal-oxide–semiconductor field-effect transistors (MOSFET) or at the interface of two semiconductors such as GaAs-GaAlAs show strong many-body effects.[2] Therefore, it has become important to study interaction effects in these systems. Accordingly, Ishihara and Kojima[3] (hereafter, IK) investigated interaction effects on the dHvA effect in these systems. They treated both the first-order exchange and correlation interactions between the electrons, but reported cancellation of the terms representing Coulomb interaction to first order in interaction.

In two dimensions a magnetic field is more effective than in three dimensions in confining electrons into Landau levels. The two conditions used by IK, that r_s is small and the magnetic field is strong, cause the electrons to be mostly in Landau levels and tend to manifest the ideal-gas behavior. Hence IK's result is understandable, but in order to find interaction effects it is desirable to relax the conditions. The present paper has been written based on this observation.

We shall treat a more interesting case in which r_s can be large and the magnetic field is not very strong under the dHvA condition. This condition requires that the field energy must be less than the Fermi energy but larger than the thermal energy. Therefore, we shall reduce the temperature first to zero before reducing the field strength; that is, the dimensionless parameter $\alpha=\beta a^2$ ($\beta=1/kT$, $a^2=\mu_B H$ is the field energy) is always large and can be infinite. We shall then be able to confirm our calculation by taking the zero-field limit. Such a limit may not be taken in the results of IK.

In addition to the two conditions, IK introduced further theoretical simplifications. First, they estimated crudely the eigenvalues of the electron propagator, obtaining a rough estimate of the correlation energy. We shall avoid such an approximation and present a precise evaluation of the eigenvalues. Second, IK determined the actual Fermi energy p_F^2, i.e., the chemical potential, as a function of the ideal Fermi energy $p_0^2=2\pi n$, by using iteration, n being

electron density. Here, and in what follows in this paper, the units are such that $\hbar=1$ and $2m=1$, m being the electron mass. As we shall discuss shortly, the Fermi energy is discontinuous at absolute zero, making applications of iterative processes based on continuity of functions undesirable.

One of the important features of the present approach is that a dimensionless parameter $\gamma_0=a^2/p_0^2$ enters in a natural way. The inverse of this parameter, γ_0^{-1}, is commonly known as the "filling factor." According to the recent study of Wilson *et al.*,[4] it is this parameter, rather than electron density itself, that is crucial in characterizing the cyclotron resonance of electrons in inversion layers. Our present treatment confirms their finding of the important role played by the filling factor.

Another important feature of the present work is that our theory becomes exact in the limit of small γ_0. Furthermore, by taking the zero-temperature limit in an appropriate way, we shall obtain the susceptibility in closed form rather than in series form as has been the case in the past.

In the next section we shall treat the ideal case in which some of the basic features of the present approach will be seen. In Sec. III we shall derive the eigenvalues of the electron propagator to be used in later sections. In consideration of the ideal case we shall evaluate the eigenvalues by splitting the domain of another important parameter $\gamma=a^2/p_F^2$, where p_F^2 is the actual Fermi energy. This split provides the key to overcome mathematical difficulties characteristic of the dHvA effect. The parameter γ is a theoretical parameter in grand ensemble theory, while γ_0 is a parameter of practical importance. Section IV deals with the first-order exchange contribution. For this purpose we shall make use of an exact sum rule. Section V will treat the ring-diagram contribution. Different from IK, we shall evaluate this contribution for both high and low densities analytically. For intermediate densities we shall employ a numerical calculation. This calculation is facilitated by a close examination of the ideal case. Since both the first-order exchange and ring contributions are treated exactly for small γ, we shall observe an exact cancellation of the first-order exchange contribution for low densities. Finally, we shall put all the contributions together to investigate interaction effects on the dHvA oscillations.

II. IDEAL GAS

According to Eq. (2.14) of IK, the grand partition function of the ideal case is given by

$$\ln\Xi_0=\frac{A\beta p_F^4}{4\pi}\left[1+\frac{\pi^2}{3\eta^2}+[(\tfrac{1}{2}g)^2-\tfrac{1}{3}]\gamma^2+\frac{4\alpha}{\eta^2}\sum_{l=1}^{\infty}(-)^{l+1}\frac{\cos(l\pi/\gamma)\cos(\frac{1}{2}gl\pi)}{l\sinh(\pi^2 l/\alpha)}\right], \tag{2.1}$$

where A is the surface area, $\beta=1/kT$, $\eta=\beta p_F^2$, $\alpha=\beta a^2$, $\gamma=a^2/p_F^2$, and g is the Lande g factor. The first two terms on the right-hand side are what we obtain even in the absence of field. The third term represents the nonoscillating field contribution in which the paramagnetic and diamagnetic parts maintain a 3 to 1 ratio as in three dimensions. The last term is the oscillating field contribution. The partition function is correct in the absence of terms of order $e^{-\eta}$ and higher.

Let us now consider the special case of $g=2$ for explicit results. Taking the zero-temperature limit, we arrive at a number-density relation in a dimensionless form as follows:

$$\frac{1}{\gamma_0}=\frac{1}{\gamma}+\frac{2}{\pi}\sum_{l=1}^{\infty}\frac{1}{l}\sin\frac{l\pi}{\gamma}\,. \tag{2.2}$$

The sinusoidal oscillations of the number density which is represented by the filling factor $1/\gamma_0=2\pi n/a^2$ are clear. The oscillations consist of an infinite number of harmonics, but the zero-

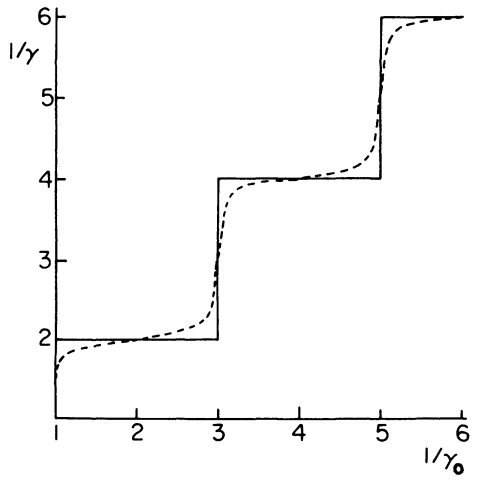

FIG. 1. Relation between the actual and ideal Fermi energies. The ordinate represents p_F^2/a^2 and the abscissa is p_0^2/a^2, where p_F^2 and p_0^2 are the actual and ideal Fermi energies, respectively, and $a^2=\mu_B H$. Solid curve: 0 K; dotted curve: 0.1 K, $H=10^4$ G (schematic).

temperature limit has resulted in a simple Fourier series. Therefore, by summing the series we arrive at

$$\frac{1}{\gamma_0}=\begin{cases}2m+1, & 2m<1/\gamma<2(m+1)\\ 2m, & 1/\gamma=2m\end{cases} \tag{2.3}$$

where m is an integer.

Although the average density n is given now explicitly as a function of $1/\gamma$, it is necessary to invert the functional relation and express $1/\gamma$ as a function of $1/\gamma_0$ because it is the latter that can be adjusted experimentally. This inverse relation is

$$\frac{1}{\gamma}=\begin{cases}2m, & 2m-1<1/\gamma_0<2m+1\\ 2m+1, & 1/\gamma_0=2m+1\ .\end{cases} \tag{2.4}$$

The variation of $1/\gamma$ as a function of $1/\gamma_0$ is illustrated in Fig. 1. As we see, $1/\gamma$ is constant about $1/\gamma_0=2m$ and jumps from $2m$ to $2(m+1)$ at $1/\gamma_0=2m+1$. $\gamma=\gamma_0$ when $1/\gamma_0$ is an integer. Hence $1/\gamma$ makes zigzag changes about the line $1/\gamma=1/\gamma_0$. Such abrupt changes are of course due to the zero-temperature limit and will be rounded off at low but finite temperatures. The dotted curve in Fig. 1 corresponds roughly to the case of $T=0.05$ K, $H=10^4$ G, and $\alpha=12.8$.

The internal energy is given by

$$U=-\left[\frac{\partial \ln \Xi_0}{\partial \beta}\right]_{\eta,A}\ . \tag{2.5}$$

We obtain for absolute zero the following result:

$$\frac{U/A}{p_F^4/4\pi}=\begin{cases}4m(m+1)\gamma^2, & 2m<1/\gamma<2(m+1)\\ 1, & 1/\gamma=2m\ .\end{cases} \tag{2.6}$$

As a function of electron density, the energy is given by

$$\frac{U/A}{p_0^4/4\pi}=\begin{cases}4m\gamma_0-4m^2\gamma_0^2\ , & \\ \qquad 2m-1<1/\gamma_0<2m+1 & \\ 4m(m+1)(2m+1)^{-2}\ , & \\ \qquad 1/\gamma_0=2m+1\ . & \end{cases} \tag{2.7}$$

Since $p_0^2=2\pi n$ with n for the number density, $p_0^4/4\pi=n(p_0^2/2)$. Hence $(U/A)/(p_0^4/4\pi)$ represents the energy per particle in the unit of $p_0^2/2$.

Similarly, the magnetization M and the susceptibility per unit area are found for $2m-1<1/\gamma_0<2m+1$ as follows:

$$\frac{M}{2N\mu_B}=2m^2\gamma_0-m\ , \tag{2.8}$$

$$\frac{\chi}{\chi_0}=2m\left[2m-\frac{1}{\gamma_0}\right]\ , \tag{2.9}$$

where N is the total number of electrons, μ_B is the Bohr magneton, and $\chi_0=(1/2\pi)(e^2/c^2)$. These physical quantities will be graphically illustrated and analyzed later in comparison with the cases with Coulomb interaction.

III. EIGENVALUES OF THE ELECTRON PROPAGATOR

We remark first that the eigenvalue expression given by Eq. (4.2) of IK is exact. In order to perform the α integration there, IK approximated the integrand function for small, intermediate, and large regions of α, estimating the dividing α. Therefore, their result is very approximate.

We have found that a new exact approach can be made by modifying the later theory of Isihara and Ioriatti (hereafter, II).[5] Let us start with their Eq. (2.5) which is also exact:

$$\lambda_j(q)=\frac{1}{2\pi}\sum_{n=1}^{\infty}(-)^{n+1}z^n\frac{\cosh(\frac{1}{2}g\alpha n)}{\sinh n\alpha}$$
$$\times\int_0^{\infty}dx\,\exp(-\pi|j|x/\alpha)\sin(Q\sin x)\exp[-Q(1-\cos x)\coth\alpha n]\ , \tag{3.1}$$

where

$$Q=q^2/\omega_0,\quad \alpha=\beta\omega_0/2,\quad \omega_0=2eH/c,\quad z=e^{\eta},\quad \eta=\beta p_F^2\ . \tag{3.2}$$

We note that the dummy summation variable n appears not only with z but also with the spin factor g. Hence it is convenient to split the spin-up and spin-down contributions from each other and write

$$\lambda_j(q)=\tfrac{1}{2}\left[\lambda_j^*\left[q,\mu+\frac{g}{4}\right]+\lambda_j^*\left[q,\mu-\frac{g}{4}\right]\right]\ . \tag{3.3}$$

If $\lambda_j^*(q)$ is evaluated, we can get both contributions easily by replacing μ by $\mu \pm g/4$.

According to Eq. (3.6) of II we have

$$\lambda_j^*(q)=\frac{1}{2\pi}\int_0^\infty \exp\left[-\frac{\pi|j|}{\alpha}x\right]\sin(Q\sin x)\sum_{k=0}^{\infty}2\Theta(k)\exp[-Q(1-\cos x)]L_k[2Q(1-\cos x)]dx\ , \tag{3.4}$$

where

$$\Theta(k)=\frac{1}{\exp[2\alpha(k+\frac{1}{2})-\eta]+1}\ . \tag{3.5}$$

At absolute zero $\Theta(k)$ is a step function:

$$\Theta(k)=\begin{cases}1, & k\le m, \epsilon_m \le p_F^2 < \epsilon_{m+1}\\ 0, & \text{otherwise}\end{cases} \tag{3.6}$$

where $\epsilon_m=(m+\frac{1}{2})\omega_0$. We can express the k sum by a contour integral

$$\sum_{k=0}^{\infty}2\Theta(k)\exp(-\tfrac{1}{2}y)L_k(y)=\frac{1}{2\pi i}\int_c dt\exp(-2^{-1}yt)g(t)=F_m(y)\ , \tag{3.7}$$

where the path c encircles 1 and

$$y=2Q(1-\cos x)\ . \tag{3.8}$$

As before, m represents an arbitrary integer and Q has been defined in Eq. (3.2).

In view of the ideal case, we evaluate $g(t)$ for restricted domains of $1/\gamma$ such that $2m-1<1/\gamma<2m+1$. The result is

$$g(t)=-1+\left[\frac{t+1}{t-1}\right]^m,\quad 2m-1<1/\gamma<2m+1 \tag{3.9}$$

in the zero-temperature limit. Hence introducing Eq. (3.9) into Eq. (3.7) we obtain

$$F_m(y)=4m\frac{J_1(X)}{X}+\frac{X^2}{24m}J_2(X)+\cdots\ ,\qquad 2m-1<1/\gamma<2m+1 \tag{3.10}$$

where

$$X=2(my)^{1/2}\ . \tag{3.11}$$

Hence for large m the higher-order terms are increasingly small.

We take the zero-temperature limit in an appropriate way. In particular, α in Eq. (3.4) shall be kept finite because it is associated with the index j of the eigenvalues. The integrand of Eq. (3.4) is large for small x so that we arrive at

$$\lambda_j^*(q)=\frac{1}{2\pi}\int_0^\infty dx\exp(-\pi|j|x/\alpha)\times\sin(Qx)F_m(c_m x) \tag{3.12}$$

$$=\frac{1}{2\pi}(1-r)+\cdots\ ,\qquad 2m-1<1/\gamma<2m+1 \tag{3.13}$$

where $c_m=(4mQ)^{1/2}$ and r is the solution of

$$s^4=\frac{8m\gamma s^2}{1-r^2}-\frac{J^2}{r^2}\ , \tag{3.14}$$

where

$$s=q/p_F,\quad J=2\pi j/\eta\ . \tag{3.15}$$

Note that, except for the restriction on γ which caused the appearance of m, the eigenvalue expression is similar to that in the absence of field. This similarity facilitates our further calculations. We also put $g=2$ for simplification.

IV. EXCHANGE EFFECTS

The exchange contribution to the grand partition function is given by a sum rule which the eigenvalues satisfy,

$$\ln\Xi_{1x}=-\frac{\beta A}{2(2\pi)^2}\int d\vec{q}[\Lambda(q)-\Lambda(0)]u(q)\ , \tag{4.1}$$

where

$$u(q)=\frac{2\pi e^2}{q}$$

is the Fourier transform of the Coulomb potential and

$$\Lambda(q)=\lim_{\beta\to\infty}\frac{1}{\beta}\sum_j\lambda_j(q)\ . \tag{4.2}$$

Since $\Lambda(q)$ is defined by a sum of the eigenvalues, we can use $\lambda_j^*(q)$ to obtain to leading order in γ the following result:

$$\Lambda(q)=\tfrac{1}{2}[\Lambda_m(q)+\Lambda_{m-1}(q)]\ ,$$
$$2(m-1)<1/\gamma<2m\ . \tag{4.3}$$

Here

$$\Lambda_m(q)=\begin{cases}p_F^2\dfrac{\kappa_m^2}{2\pi}\left[1-\dfrac{2}{\pi}\cos^{-1}s_m+\dfrac{2}{\pi}s_m(1-s_m^2)^{1/2}\right], & s_m\le 1\\ p_F^2\dfrac{\kappa_m^2}{2\pi}, & s_m\ge 1\end{cases} \tag{4.4}$$

where

$$\kappa_m=(2m\gamma)^{1/2},\quad s_m=s/(2\kappa_m)\ . \tag{4.5}$$

The corrections to the result in Eq. (4.4) are of order $O(p_F^2\kappa_m^2\gamma^2)$ or higher. Note that the combination of p_F^2 with κ_m^2 characterizes $\Lambda(q)$.

The exchange contribution shall be combined with the ring-diagram contribution. It is canceled out by a term in the ring-diagram contribution for low densities, as will be shown in the next section.

The exchange contribution to the grand partition function is given to lowest order in γ by

$$\ln\Xi_{1x}=\frac{2\beta Ae^2}{3\pi^2}\frac{(p_F\kappa_m)^3+(p_F\kappa_{m-1})^3}{2},\quad 2(m-1)<1/\gamma<2m \tag{4.6}$$

Note that the grand partition function does not explicitly depend on η. This turns out to be so to all orders in γ. Hence the first-order exchange contribution will not change the number-density relation of Eq. (2.2).

The first-order exchange contribution to the internal energy is given to leading order in γ by

$$\frac{U_{1x}/A}{p_F^4/4\pi}=-\frac{8\sqrt{2}}{3\pi}\frac{\kappa_m^3+\kappa_{m-1}^3}{2}\left[\frac{\gamma}{\gamma_0}\right]^{1/2}r_s,\quad 2(m-1)<1/\gamma<2m \tag{4.7}$$

where

$$r_s=e^2/\sqrt{2}p_0,\quad \gamma_0=a^2/p_0^2\ . \tag{4.8}$$

In the absence of a magnetic field, the energy is reduced to the known result, in rydbergs,

$$\frac{U_{1x}^0/A}{p_0^2/2\pi}=\frac{U_{1x}^0}{N}=-\frac{e^4}{4}\frac{8\sqrt{2}}{3\pi}\frac{1}{r_s}=-\frac{1.2004}{r_s}\ . \tag{4.9}$$

It is easy to prove that the corrections to the result in Eq. (4.6) or (4.7) are smaller by the factor γ^2. One can rewrite Eq. (4.7) in terms of p_0^2 rather than p_F^2 by making use of

$$\left[\frac{\gamma_0}{\gamma}\right]^2=\begin{cases}\left[\left[\dfrac{2m}{2m+1}\right]^2,\left[\dfrac{2(m+1)}{2m+1}\right]^2\right], & \gamma_0=2m+1\\ [2(m+1)]^2\gamma_0^2, & 2m+1<1/\gamma_0<2m+3\end{cases} \tag{4.10}$$

and also

$$\frac{U_{1x}/A}{p_F^4/4\pi}=-r_s^*\frac{(2m)^{3/2}+[2(m+1)]^{3/2}}{2}\frac{\gamma^2}{\gamma_0^{1/2}},\quad 2m<1/\gamma<2(m+1) \tag{4.11}$$

where

$$r_s^* = \frac{8\sqrt{2}}{3\pi} r_s \ . \tag{4.12}$$

In concluding this section, we list relevant formulas for the internal energy, magnetization, and magnetic susceptibility which are correct to the first-order exchange contribution and to lowest order in γ_0:

$$\frac{U/A}{p_0^4/4\pi} = 4u_1 m\gamma_0 - 4u_2 m^2\gamma_0^2, \quad 2m-1 \le 1/\gamma_0 < 2m+1 \ , \tag{4.13}$$

where

$$u_1 = 1 + \frac{\sqrt{2}}{3\pi} r_s(2m) \left\{ \left[\frac{2m-1}{2m} \right]^{1/2} \left[1 + \left[\frac{m-1}{m} \right]^{3/2} \right] - \left[\frac{2m+1}{2m} \right]^{1/2} \left[1 + \left[\frac{m+1}{m} \right]^{3/2} \right] \right\}$$

$$= 1 + \Delta u_1 \ , \tag{4.14}$$

$$u_2 = 1 + \frac{2\sqrt{2}}{3\pi} r_s(2m) \left\{ \left[\frac{2m+1}{2m} \right] \left[\frac{2m-1}{2m} \right]^{1/2} \left[1 + \left[\frac{m-1}{m} \right]^{3/2} \right] - \left[\frac{2m-1}{2m} \right] \left[\frac{2m+1}{2m} \right]^{1/2} \left[1 + \left[\frac{m+1}{m} \right]^{3/2} \right] \right\}$$

$$= 1 + \Delta u_2 \ . \tag{4.15}$$

Note that in the high-density limit $u_1 = u_2 = 1$, while for $m \to \infty$

$$\Delta u_1 = \Delta u_2 = -\frac{8\sqrt{2}}{3\pi} r_s \ . \tag{4.16}$$

The magnetization M and susceptibility (per unit area) are given by

$$\frac{M/A}{2\mu_B n} = 2(1+\Delta u_2) m^2 \gamma_0 - (1+\Delta u_1) m \ , \tag{4.17}$$

$$\frac{\chi}{2\chi_0} = 2(1+\Delta u_2) m^2 - (1+\Delta u_1) \frac{m}{\gamma_0} \ , \tag{4.18}$$

where $\chi_0 = e^2/2\pi c^2$ as before, and $2m-1 < 1/\gamma_0 < 2m+1$.

V. RING-DIAGRAM CONTRIBUTION

The ring-diagram contribution to the grand partition function is given in terms of the eigenvalues also,

$$\ln \Xi_r = \frac{A}{2(2\pi)^2} \int d\vec{q} \sum_j \{ u(q) \lambda_j(q) - \ln[1 + u(q)\lambda_j(q)] \} \ . \tag{5.1}$$

We evaluate the grand partition function for specified intervals of γ. The eigenvalues as a sum of the spin-up and spin-down parts can be given to order γ by

$$\lambda_j(q) = \tfrac{1}{2}[\lambda_j(q, m-1) + \lambda_j(q,m)], \quad 2(m-1) < 1/\gamma < 2m$$

$$\approx \lambda_j(q, m - \tfrac{1}{2}), \quad 2(m-1) < 1/\gamma < 2m \tag{5.2}$$

$$\lambda_j(q,m) = \lambda_j^*(q) \ , \tag{5.3}$$

where $\lambda_j^*(q)$ is defined by Eq. (3.12).

For absolute zero, it is appropriate to replace the sum over j by integration. The convenient variable is

$$z = \frac{\pi j}{Q\alpha} = \frac{2\pi j}{\beta q^2} \ .$$

We introduce also a new variable ρ_m defined by

$$\rho_m=\frac{2p_F\kappa_m}{q} \tag{5.4}$$

and then transform the set of variables (z,ρ_m) into a new set (ξ_m,ϕ_m) in accordance with

$$\rho_m=\cosh\xi_m \sin\phi_m \ , \tag{5.5}$$
$$|z|=\sinh\xi_m \cos\phi_m \ .$$

To first order in γ we can use Eq. (3.13) to arrive at a simple expression

$$\lambda_j(q,m)=\frac{1}{2\pi}(1-\cos\phi_m) \ . \tag{5.6}$$

The ξ integration in $\ln\Xi_r$ can be carried out, leading to

$$\ln\Xi_r=-\beta A\frac{e^4}{4}\left[\frac{2p_F\kappa}{\pi}\right]^2\int_0^{\pi/2}d\phi(\cos\phi-\cos2\phi)(1-\cos\phi)\sin\phi \times\left[\left[\frac{\pi}{2}-x(\phi)F(x(\phi))\right]I_5(\phi) -\left[\frac{\pi}{4}-x(\phi)+\frac{\pi}{2}x^2(\phi)-x^3(\phi)F(x(\phi))\right]I_3(\phi)\right] , \quad [2(m-1)<1/\gamma<2m] \tag{5.7}$$

where

$$x(\phi)=\tilde{r}_s(1-\cos\phi)\sin\phi \ , \tag{5.8}$$

$$\tilde{r}_s=\frac{e^2}{2p_F\kappa}=r_s\frac{(\gamma/\gamma_0)^{1/2}}{2^{1/2}\kappa}, \quad \kappa=[(2m-1)\gamma]^{1/2} , \tag{5.9}$$

$$F(x)=\int_0^\infty d\xi\frac{1}{1+x\cosh\xi} \ , \tag{5.10}$$

$$I_3(\phi)=-\frac{\cos\phi}{2\sin^2\phi}+\tfrac{1}{2}\ln\left[\tan\frac{\phi}{2}\right] , \tag{5.11}$$

$$I_5(\phi)=-\frac{\cos\phi}{4\sin^4\phi}+\tfrac{3}{8}\left[\ln\left[\tan\frac{\phi}{2}\right]-\frac{\cos\phi}{\sin^2\phi}\right] . \tag{5.12}$$

Note that the grand partition function depends on the combination of p_F with κ. Therefore, it will not contribute to the number density; that is, the Fermi energy will stay as in the ideal case.

The integral $F(x)$ is tabulated for $x\lesssim 1$. Note that the variable x is proportional to $\tilde{r}_s$ as in Eq. (5.8) and that no small momentum-transfer approximation has been used, that is, Eq. (5.7) is exact. We now consider high- and low-density cases separately.

A. High density

For high density, x is small and we find

$$F(x)=-\ln\frac{x}{2}+O(x^2\ln x) \ . \tag{5.13}$$

Introducing Eq. (5.13) into Eq. (5.7) and carrying out the ϕ integration we arrive at

$$\ln\Xi_r=-\beta nA\frac{e^4}{4}\kappa_0^2(R_0+R_1\tilde{r}_s\ln\tilde{r}_s+R_2\tilde{r}_s) \ , \tag{5.14}$$

where

$$R_0=-0.6137, \quad \kappa_0=[(2m-1)\gamma_0]^{1/2} ,$$
$$R_1=-0.2441, \quad \tilde{r}_s=\frac{r_s}{\sqrt{2}\kappa}\left[\frac{\gamma}{\gamma_0}\right]^{1/2} , \tag{5.15}$$
$$R_2=1.139 \ .$$

The ring-diagram contributions to the internal en-

ergy and susceptibility are given by

$$\frac{U_r/A}{p_F^4/4\pi}=(2m-1)\gamma^2 x_r \times(R_0+R_1\tilde{r}_s\ln\tilde{r}_s+R_2\tilde{r}_s)\,, \tag{5.16}$$

$$\frac{\chi_r}{\chi_0}=-\frac{2m-1}{2}x_r \times\left[R_0+\frac{R_1}{2}\tilde{r}_s\ln\tilde{r}_s+\frac{R_2-R_1}{2}\tilde{r}_s\right], \tag{5.17}$$

where $2(m-1)<1/\gamma<2m$ and $x_r=e^4/2a^2$.

B. Low density

In low density, i.e., $\tilde{r}_s\geq 1$, $x(\phi)$ is large. The function $F(x)$ is expanded as follows:

$$F(x)=\frac{1}{x}\sum_{n=0}^{\infty}\frac{(-)^n}{n!x^n}2^{n-1}\left[\Gamma\left[\frac{n+1}{2}\right]\right]^2. \tag{5.18}$$

The grand partition function can be given rigorously in terms of a Mellin transform in the following form:

$$\ln\Xi_r=-\beta A\frac{e^4}{4}\left[\frac{2p_F\kappa}{\pi}\right]^2\frac{\pi^{3/2}}{2}\frac{1}{2\pi i} \times\int_{c-i\infty}^{c+i\infty}\frac{(\tilde{r}_s)^{-s}}{(s-2)\sin\pi s}\frac{\Gamma\left[\frac{1+s}{2}\right]}{\Gamma\left[1+\frac{s}{2}\right]}I(s)\,, \tag{5.19}$$

where $2(m-1)<1/\gamma<2m$ and

$$I(s)=\int_0^{\pi/2}\frac{d\phi}{[\sin\phi(1-\cos\phi)]^{s-2}} \times\left[\frac{1}{\sin^5\phi}-\frac{s+1}{s+2}\frac{1}{\sin^3\phi}\right]. \tag{5.20}$$

Note that Eq. (5.19) represents a rigorous analytical continuation into low-density regions: The high- and low-density expressions for the grand partition function hinge upon the change in the analytical character of $F(x)$ which takes place at $x=1$. After a straightforward calculation we arrive at

$$\ln\Xi_r=\beta nA\frac{e^4}{4}\kappa_0^2\left[\frac{L_0}{\tilde{r}_s^{2/3}}+\frac{L_1}{\tilde{r}_s}+\frac{L_2}{\tilde{r}_s^{4/3}}+\cdots\right], \quad 2(m-1)<1/\gamma<2m \tag{5.21}$$

where

$$L_0=\frac{2\pi^2}{[\Gamma(1/3)]^3}=1.0267\,,$$

$$L_1=-\frac{8}{3\pi}=-0.848\,83\,,$$

$$L_2=\frac{\sqrt{3}[\Gamma(1/3)]^3}{120\pi}=0.088\,328\,.$$

Under the same approximation as for Eq. (5.2) we find for $2(m-1)<1/\gamma<2m$

$$\ln\Xi_{1x}=-\beta nA\frac{e^4}{4}\kappa_0^2\frac{L_1}{\tilde{r}_s}\,. \tag{5.22}$$

Hence the second term in Eq. (5.21) cancels precisely this first-order exchange contribution. Note that the right-hand side of Eq. (5.21) represents essentially the ground-state energy for large r_s,

$$\frac{U_r/A}{p_F^4/4\pi}=-\frac{U_{1x}/A}{p_F^4/4\pi} -x_r(2m-1)\gamma^2\left[\frac{L_0}{\tilde{r}_s^{2/3}}+\frac{L_2}{\tilde{r}_s^{4/3}}\right], \quad 2(m-1)<1/\gamma<2m \tag{5.23}$$

where $x_r=e^4/2a^2$ as before.

VI. RESULTS AND DISCUSSION

We have evaluated the grand partition function in consideration of the first-order exchange and ring contributions. For the latter we have obtained both the high- and low-density results. Our evaluation has been facilitated by splitting the domain of γ such that $2m<1/\gamma<2(m+1)$. We have observed that both exchange and ring grand partition functions are determined by $p_F\kappa_m$ or $p_F\kappa$ rather than by p_F itself. Therefore, the number-density relation will not be changed from the ideal-gas case. Therefore, no change in the period of the dHvA oscillations is expected. This is in conformity with what Kohn observed some years ago.[6]

Assembling all these contributions we obtain the total energy as follows.

A. High density [$2m<1/\gamma<2(m+1)$]

We have

$$\frac{U/A}{p_F^4/4\pi}=\{4m(m+1)-r_s^*(2m+1)^{3/2}\gamma_0^{-1/2}+a_1(2m+1)\gamma_0^{-1}+a_2(2m+1)^{1/2}\gamma_0^{-3/2} +a_3(2m+1)^{1/2}\gamma_0^{-3/2}\ln[(2m+1)\gamma_0]\}\gamma^2\,, \tag{6.1}$$

where r_s^* has been defined by Eq. (4.12) and

$$a_1=R_0 r_s^2,\quad a_2=\frac{r_s^3}{\sqrt{2}}(R_1\ln r_s+R_2-R_1\ln\sqrt{2}),\quad a_3=-\frac{R_1}{2\sqrt{2}}r_s^3 . \tag{6.2}$$

The R's are defined in Eq. (5.15).

B. Low density $[2m<1/\gamma<2(m+1)]$

We have

$$\frac{U/A}{p_F^4/4\pi}=\left[4m(m+1)-x_r(2m+1)\left[\frac{L_0}{r_s'^{2/3}}+\frac{L_2}{r_s'^{4/3}}\right]\right]\gamma^2, \tag{6.3}$$

where

$$x_r=e^4/2a^2,\quad r_s'=\frac{e^2}{2a(2m+1)^{1/2}}=\frac{r_s}{\sqrt{2}[(2m+1)\gamma_0]^{1/2}} . \tag{6.4}$$

The calculation has been based on small γ or large m. For practical purposes the γ^{-1} interval should be changed into that for γ_0^{-1} based on Eq. (2.3). We find then for the interval $2m-1<1/\gamma_0<2m+1$ the following result:

$$\frac{U/A}{p_0^4/4\pi}=4[1+f(r_s)]m\gamma_0-4\left[1+\frac{(2m-1(2m+1)}{(2m)^2}f(r_s)\right]m^2\gamma_0^2 , \tag{6.5}$$

where the function $f(x)$ is given by

$$f(x)=\begin{cases}x^2\left[-\dfrac{1.2004}{x}-0.6137-0.1726x\ln x+0.8653x+\cdots\right], & x<1 \quad (6.6a)\\ x^2\left[-\dfrac{1.2935}{x^{2/3}}-\dfrac{0.14018}{x^{4/3}}+\cdots\right], & x>1 . \quad (6.6b)\end{cases}$$

Note that $f(r_s)$ is equal to r_s^2 [(ground-state energy minus kinetic energy) in the absence of field] for high and low densities. Hence we might suspect whether the same relation holds even in the intermediate densities. That this is indeed the case can be proved easily by using Eqs. (5.22) and (5.7) with the help of Eq. (2.3). Therefore, our final result, which is correct to order γ_0, is

$$\frac{U/A}{p_0^4/4\pi}=4[1+r_s^2\epsilon(r_s)]m\gamma_0 -4\left[1+\frac{(2m-1)(2m+1)}{(2m)^2}r_s^2\epsilon(r_s)\right]m^2\gamma_0^2 . \tag{6.7}$$

Hence the magnetization is

$$\frac{M/A}{2\mu_B n}=2\left[1+\frac{(2m-1)(2m+1)}{(2m)^2}r_s^2\epsilon(r_s)\right]m^2\gamma_0 -[1+r_s^2\epsilon(r_s)]m . \tag{6.8}$$

The susceptibility is obtained from

$$\frac{\chi}{\chi_0}=\frac{M/A}{\gamma_0\mu_B n} . \tag{6.9}$$

All these formulas are restricted to $2m-1<1/\gamma_0<2m+1$. In Eq. (6.8)

$$\epsilon(r_s)=-\frac{8\sqrt{2}}{3\pi}\frac{1}{r_s}+\frac{8}{\pi}\Phi \tag{6.10}$$

[where Φ is the ϕ integral of Eq. (5.7) in which $\tilde{r}_s$ is replaced by r_s] is the sum of the first-order exchange and ring-diagram contributions to the ground-state energy in the absence of field.

In $\epsilon(r_s)$ the ring contribution is important for all densities. However, in the neglect of higher-order exchange contributions, it is safe to limit our results to small r_s of order 1. Nevertheless, we remark that Ferrell's condition[7]

$$\frac{d^2}{dr_s^2}[r_s^2\epsilon(r_s)]\le 0$$

is satisfied for all r_s. Since $\epsilon(r_s)$ decreases in proportion to $-r_s^{-2/3}$ for large r_s, it is easy to see that

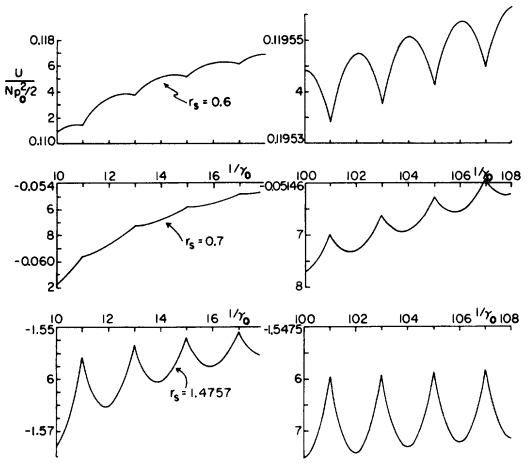

FIG. 2. Internal energy per particle in the unit of $p_0^2/2$ as a function of $\gamma_0^{-1}=p_0^2/a^2$, where $p_0^2=2\pi n$ and $a^2=\mu_B H$. The curves from top to bottom correspond respectively to $r_s=0.6$, 0.7, and 1.4757. The right-side curves represent the cases in which $1/\gamma_0$ is large.

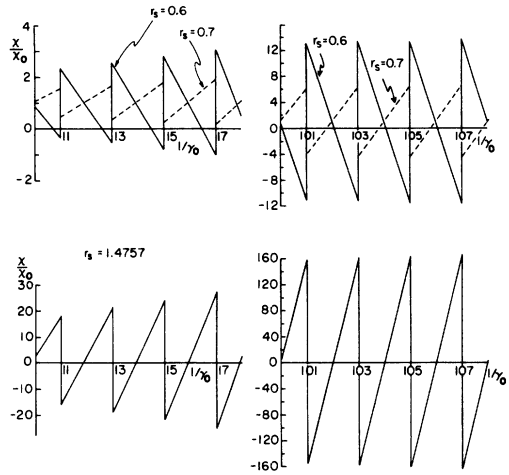

FIG. 4. Susceptibility of interacting electron systems. An inversion of the oscillations takes place at around $r_s=0.7$.

the above inequality is satisfied.

The internal energy U is illustrated in Fig. 2 in the dimensionless form of Eq. (6.5) as a function of the filling factor $1/\gamma_0$ in the vicinity of the point at which $\epsilon(r_s)$ vanishes. The left-side graphs correspond to smaller γ_0^{-1} than those on the right side. The top curves corresponding to $r_s=0.6$ are similar to the ideal case. The energy U shows parabolic changes, the average of which approach gradually $Np_0^2/2$, N being the total number of electrons. Hence the oscillations on the right side have very small amplitudes despite their appearance in the graph. These oscillations are larger for smali r_s, that is, they are suppressed by Coulomb interaction. The middle curves represent this suppression. At $r_s\sim 0.7$ the ground-state energy vanishes. Accordingly, the internal energy shows very little change, and then varies concavely downward, as shown more clearly in the bottom curves which correspond to $r_s=1.4757$. Note that the oscillations are somewhat clearer than the case of $r_s=0.7$, around which the interesting inversion of the oscillating pattern takes place. Note that in all these cases the periodicity remains the same. Note also that the cusps representing minima ($r_s<0.7$) or maxima ($r_s>0.7$) of the internal energy appear whenever $1/\gamma_0$ is an odd integer.

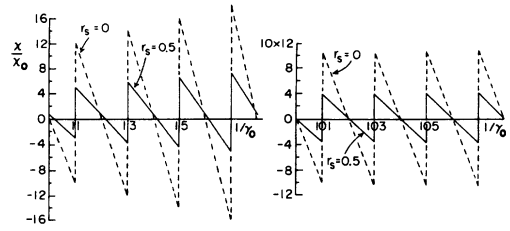

FIG. 3. Susceptibility of the ideal case (dotted lines) is compared with that corresponding to the case of $r_s=0.5$. The zigzag changes are suppressed by Coulomb interaction for small r_s. The right-side graph corresponds to larger values of the abscissa.

Because the energy is parabolic, the magnetization curves are almost straight. Since these curves are similar to those of the susceptibility, we have omitted their illustrations.

The ideal susceptibility in the unit of χ_0 is illustrated in Fig. 3 by dotted lines. The susceptibility shows prominent zigzag changes. These changes are rounded off at finite temperatures, but the basic features of the oscillations will be preserved. Note that the susceptibility jumps at the odd integral $1/\gamma_0$, and also that the peak values are even integers. Hence the peak values increase as $1/\gamma_0$ increases. The right-side dotted lines show such a variation. The solid lines corresponding to $r_s=0.5$ have been obtained from the high-density series of Eq. (6.6a). Note that the oscillations are suppressed by interaction and also that on the left side the susceptibility does not vanish precisely at the even integral $1/\gamma_0$. As $1/\gamma_0$ increases, however, this deviation gradually disappears and only the amplitude suppression remains. In spite of these deviations, the overall features of the oscillations are the same as those of the ideal case.

Figure 4 illustrates the important changes which take place around the point where the energy $\epsilon(r_s)$ vanishes. The solid lines corresponding to $r_s=0.6$ still show the ideal-gas characteristics. However,

the dotted lines for $r_s=0.7$ show opposite zigzag variations, due to the change in the sign of the ground-state energy $\epsilon(r_s)$. These opposite oscillations may be considered to be characteristic of a liquid state as they become enhanced, rather than suppressed, by Coulomb interaction. The bottom curves in Fig. 4 illustrate this trend clearly.

In all these cases, the amplitude of the oscillations is increasing for larger $1/\gamma_0$. However, it is probably more difficult to make observations at large $1/\gamma_0$ because the oscillations become very rapid.

It is known that the ground-state energy becomes negative due to Coulomb interaction. Indeed, the exchange and correlation contributions have been considered important for metallic cohesion. It is known also that electrons will eventually form a crystalline lattice. Since the lattice energy is negative and the gas energy is positive, the ground-state energy must vanish at a certain point if a single energy function represents both phases. According to our present analysis, this takes place at around $r_s=0.7$ where the field effects on the system show significant changes. Such changes are interesting and await experimental tests.

ACKNOWLEDGMENT

This work was supported by the ONR under Contract No. N00014-79-C-0451.

[1]L. Onsager, Philos. Mag. 43, 1006 (1952); I. M. Lifshitz and A. M. Kosevich, Zh. Eksp. Teor. Phys. 29, 730 (1955) [Sov. Phys.—JETP 2, 636 (1956)]; A. Isihara, J. Tsai, and M. Wadati, Phys. Rev. A 3, 990 (1971); F. C. Alkarez, Y. Kojima, and A. Isihara, J. Phys. Chem. Solids 40, 846 (1979).

[2]See for instance, T. Ando, A. B. Fowler, and F. Stern, Rev. Mod. Phys. 54, 437 (1982).

[3]A. Isihara and D. Y. Kojima, Phys. Rev. B 19, 846 (1979).

[4]B. A. Wilson, S. J. Allen, Jr., and D. C. Tsui, Phys. Rev. Lett. 44, 479 (1980).

[5]A. Isihara, L. Ioriatti, Jr., and D. Y. Kojima, Z. Phys. B 44, 91 (1981); L. Ioriatti, Jr. and A. Isihara, *ibid.* 44, 1 (1981).

[6]W. Kohn, Phys. Rev. 123, 1242 (1961).

[7]R. A. Ferrell, Phys. Rev. Lett. 1, 443 (1958).